

Supporting Information

Dual-light defined *in situ* oral mucosal lesions therapy through a mode switchable anti-bacterial and anti-inflammatory mucoadhesive hydrogel

Huijie Liu^{a,c}, Qun Li^{a,c}, Yingying Xu^{a,c}, Yue Sun^b, Xin Fan^a, Huaqiang Fang^c, Binbin Hu^c, Li Huang^c, Lan Liao^{*a}, and Xiaolei Wang^{*b,c}

^a The Affiliated Stomatological Hospital of Nanchang University, The Key Laboratory of Oral Biomedicine, Jiangxi Province Clinical Research Center for Oral Diseases, Nanchang University, Nanchang, Jiangxi, 330006, P.R. China. E-mail: liaolan5106@ncu.edu.cn.

^b College of Chemistry and Chemical Engineering of Nanchang University, Nanchang University, Nanchang, Jiangxi, 330088, P.R. China. E-mail: wangxiaolei@ncu.edu.cn.

^c The National Engineering Research Center for Bioengineering Drugs and the Technologies Institute of Translational Medicine, Nanchang University, Nanchang, Jiangxi, 330088, P.R. China.

*Corresponding authors

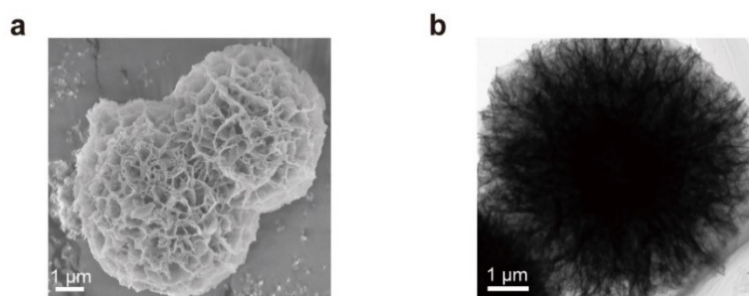


Figure S1. SEM image (a) and TEM image (b) of ZnO.

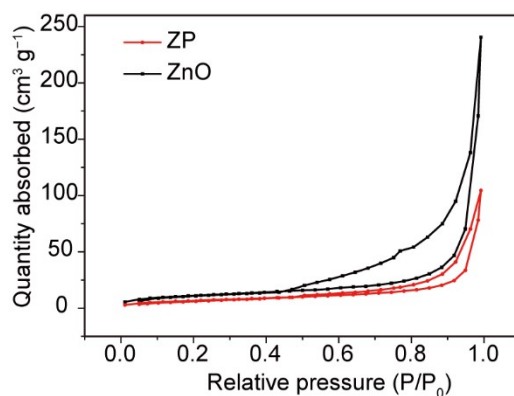


Figure S2. N₂ adsorption-desorption analysis of ZnO and ZP.

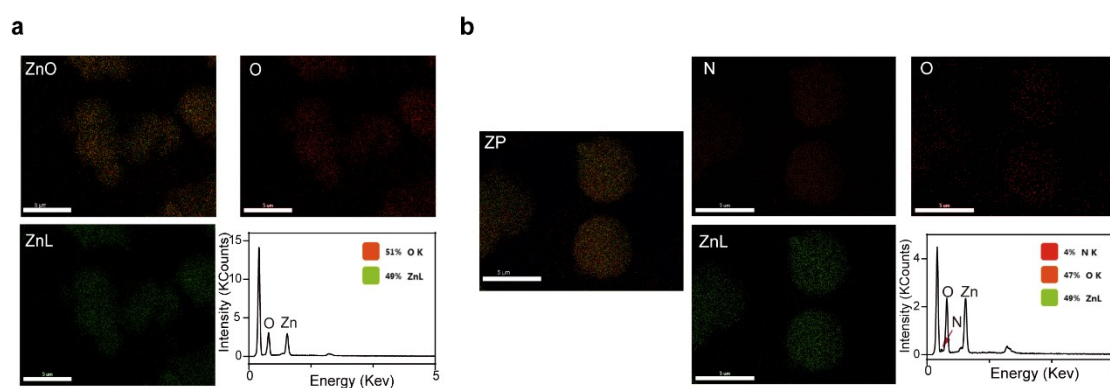


Figure S3. EDS spectra of ZnO (a) and ZP (b).

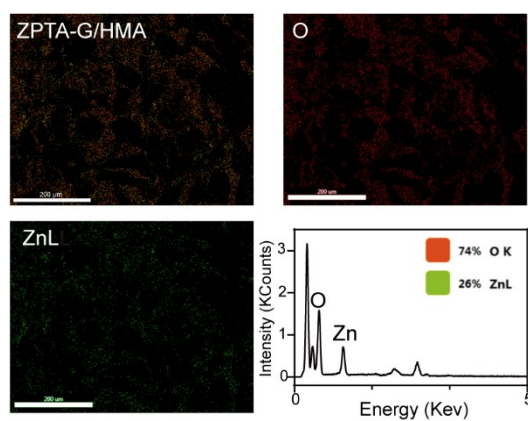


Figure S4. EDS spectrum of ZPTA-G/HMA.

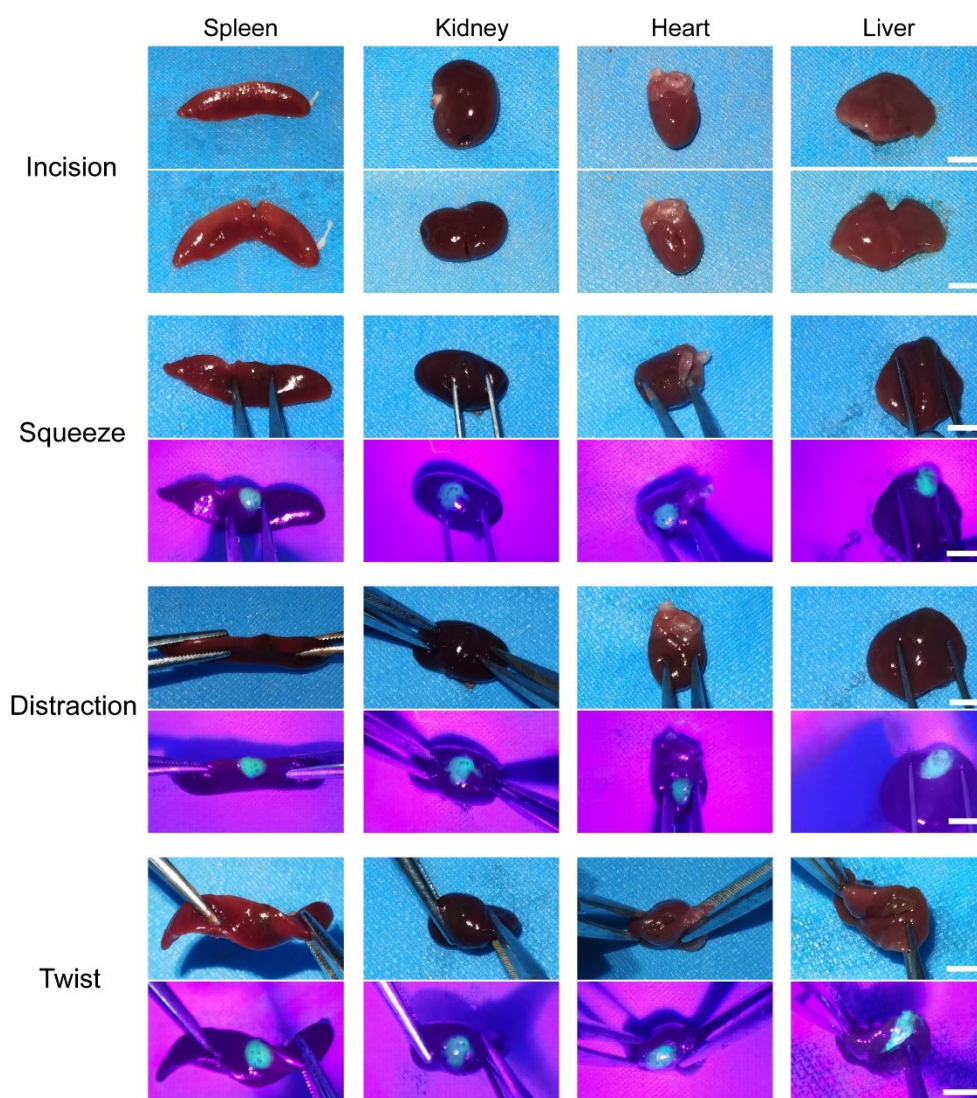


Figure S5. ZPTA-G/HMA was taken to bond the incisions on fresh rat vital organs (spleen, liver, kidney and heart). The bonding strength could resist the squeeze, distraction and twist by external forces. Scale bar = 1 cm.

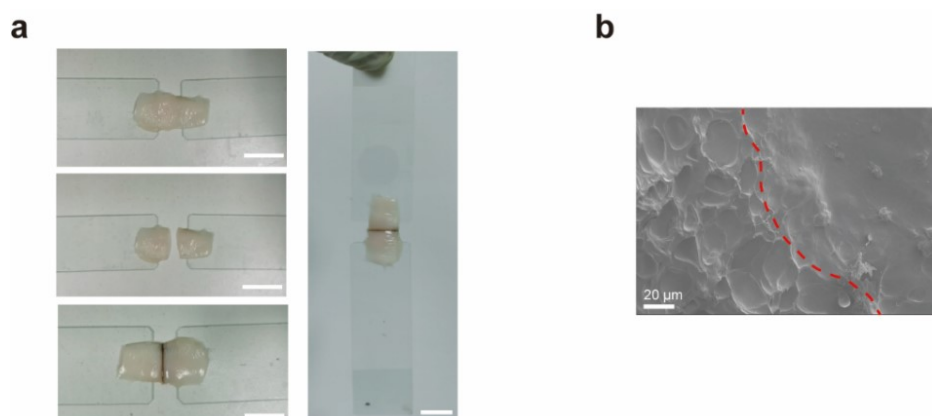


Figure S6. (a) ZPTA-G/HMA was taken to bond the incisions on fresh porcine gingiva mucosa. Scale bar = 1 cm. (b) SEM image of the integration of the ZPTA-G/HMA with porcine gingiva mucosa (red dashed line indicates the boundary).

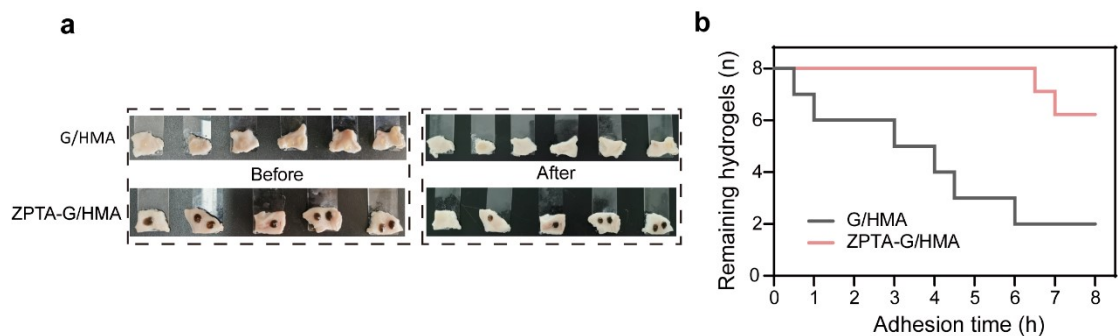


Figure S7. (a) Representative photographs of the adhesion of G/HMA and ZPTA-G/HMA after artificial saliva impingement at 1400 rpm within 8 h. (b) Corresponding number of residual ZPTA-G/HMA and G/HMA as a function of time.

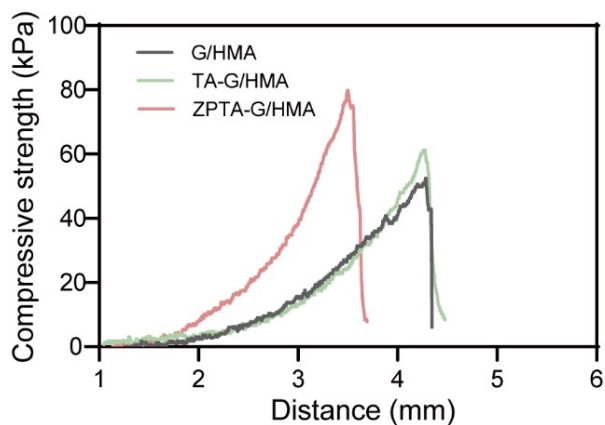


Figure S8. Force-distance curves of G/HMA, TA-G/HMA and ZPTA-G/HMA.

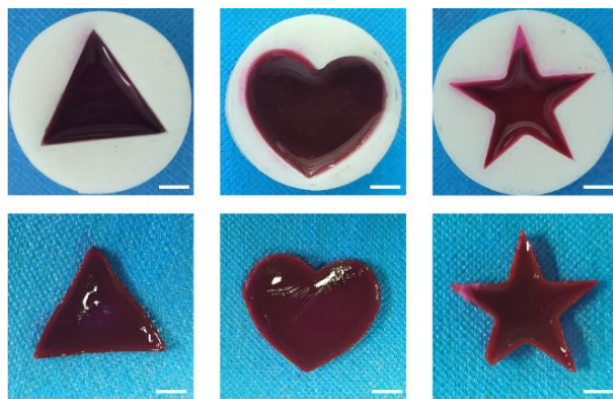


Figure S9. Evaluation of the plasticity of ZPTA-G/HMA. ZPTA-G/HMA behaved as a thin film that could be adapted to different shapes. Scale bar = 0.25 cm.

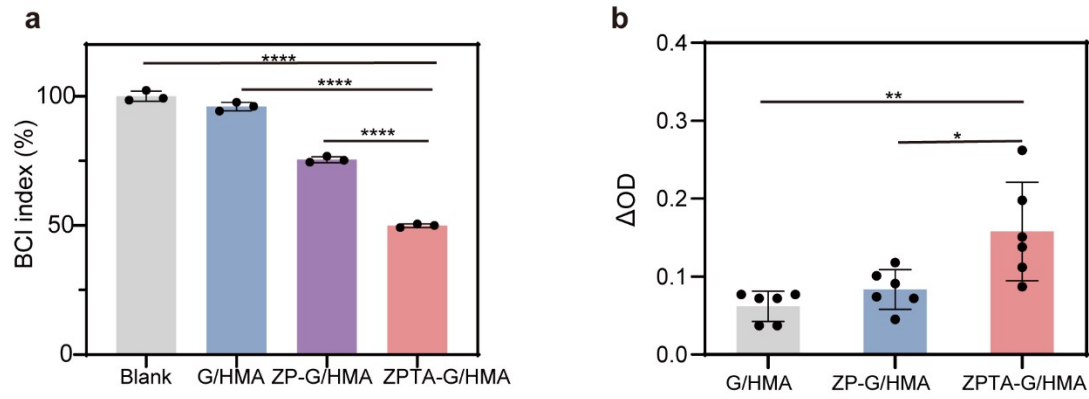


Figure S10. *In vitro* hemostasis assay. (a) BCl of the Blank group, G/HMA, ZP-G/HMA and ZPTA-G/HMA. (b) BSA adsorption in the surface of the G/HMA, ZP-G/HMA and ZPTA-G/HMA. Data are means \pm s.d. ($n \geq 3$). * $p < 0.05$, ** $p < 0.01$, **** $p < 0.0001$.

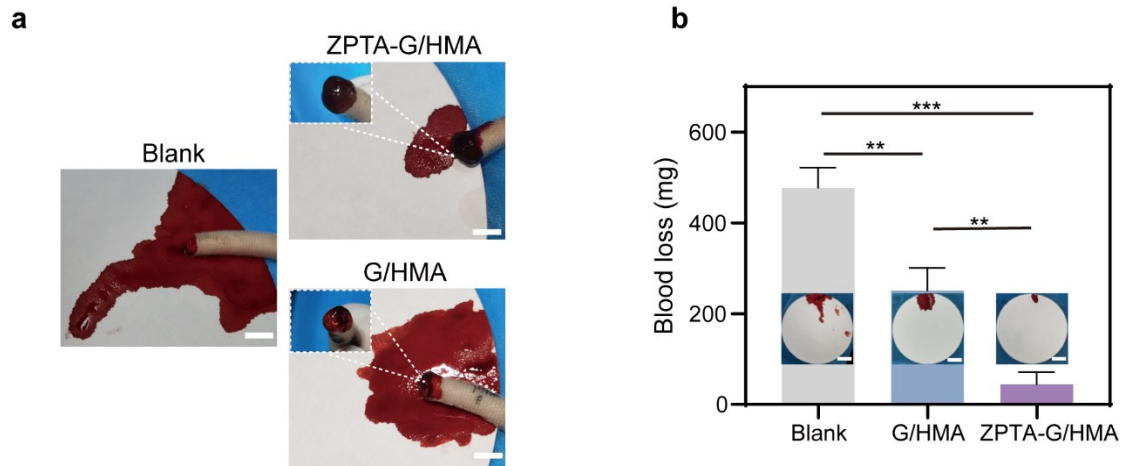


Figure S11. *In vivo* hemostasis assay. (a) Rat tail amputation with different treatments. Scale bar = 1 cm. (b) The corresponding quantification of blood loss. Scale bar = 2 cm. ** $p < 0.01$, *** $p < 0.001$. Data are means \pm s.d. ($n \geq 3$).

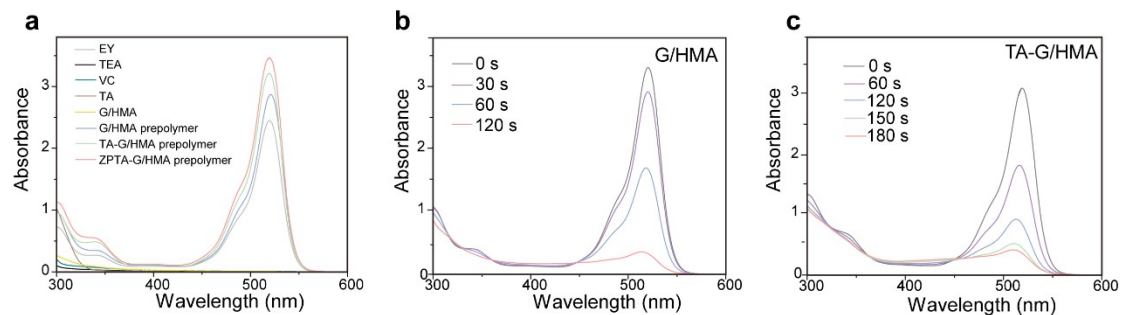


Figure S12. (a) UV-vis absorption spectra of TEA, VC, EY, TA, G/HMA, G/HMA prepolymer, TA-G/HMA prepolymer and ZPTA-G/HMA prepolymer. Concentration of TEA, VC, EY, GelMA, HAMA, TA, ZP was 1.88% (w/v), 1.25% (w/v), 0.5 mM, 15% (w/v), 2% (w/v), 200 $\mu\text{g mL}^{-1}$, 1% (wt%), respectively. (b-c) UV-vis absorption spectra of G/HMA and TA-G/HMA at different times under GL irradiation.

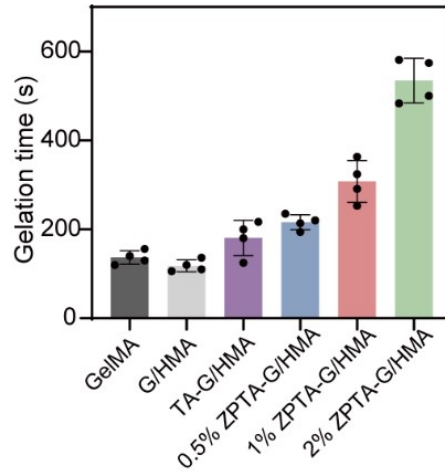


Figure S13. Gelation time of different samples under GL irradiation. Data are means \pm s.d. ($n \geq 3$).

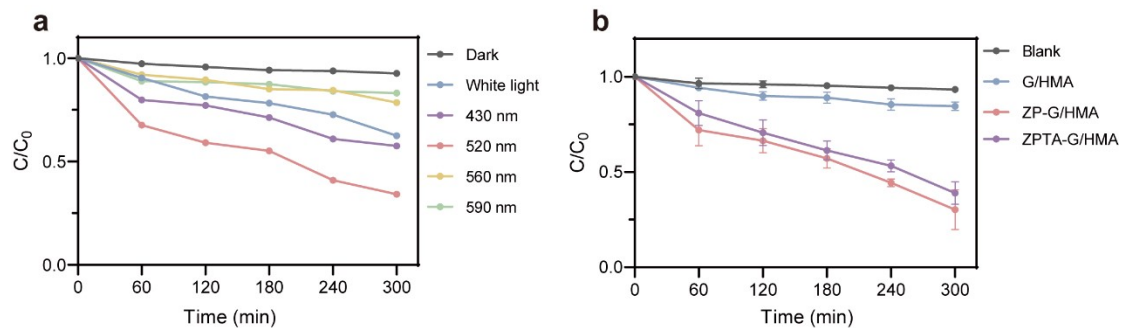


Figure S14. (a) Degradation rates of RhB by ZPTA-G/HMA under different wavelengths of light conditions. (b) Degradation rates of RhB by different samples under GL irradiation.

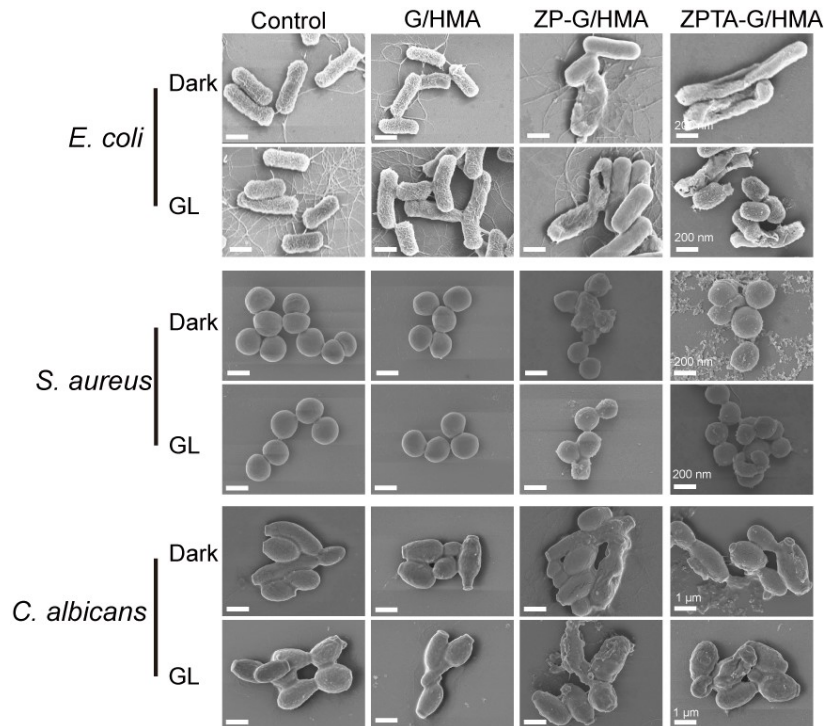


Figure S15. SEM images of bacteria co-cultured with different samples with/without

GL irradiation as referred to Figure 3h.

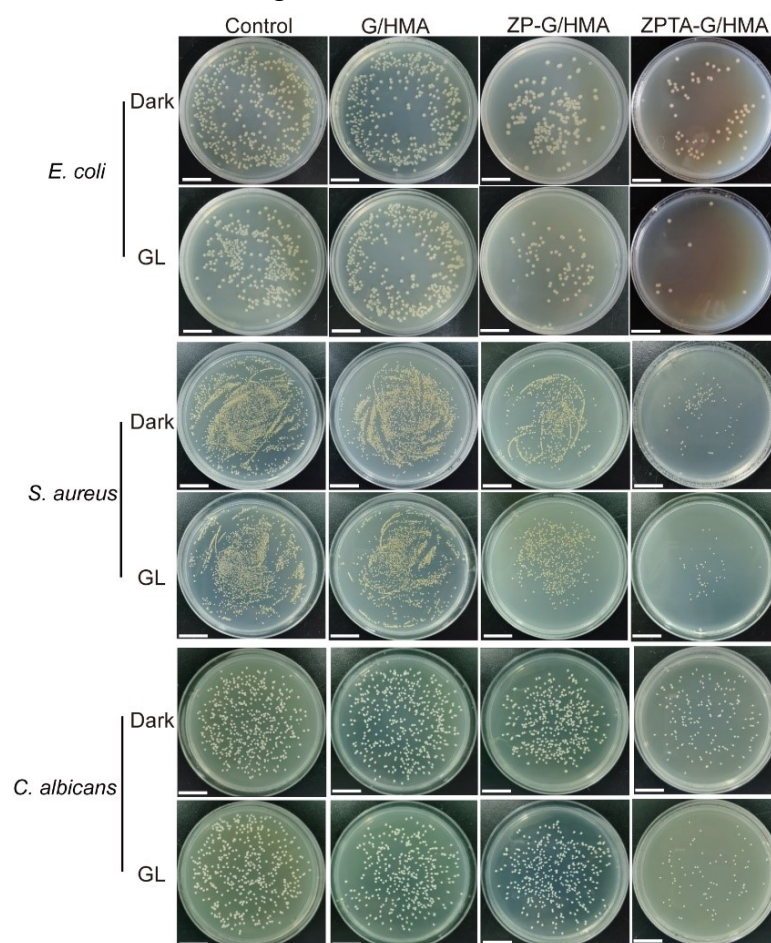


Figure S16. Agar plates photos of *E. coli*, *S. aureus* and *C. albicans* as referred to Figure 3g. Scale bar = 2 cm.

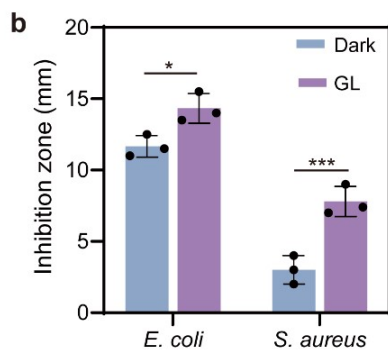
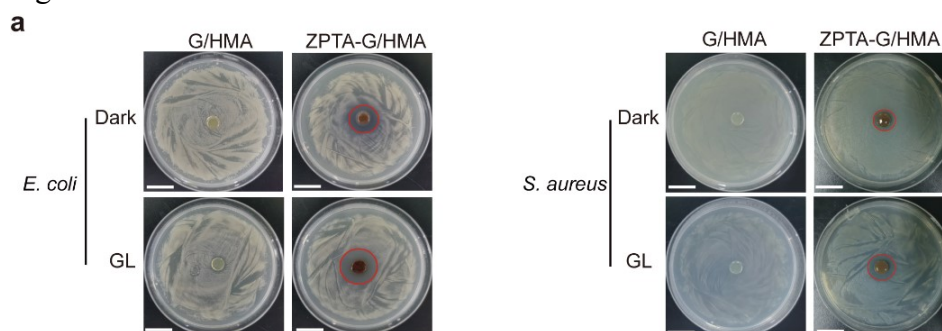


Figure S17. The photos (a) and the sizes (b) of inhibition zone of G/HMA and ZPTA-

G/HMA with/without GL irradiation. Scale bar = 2 cm. Data are means \pm s.d. ($n \geq 3$).
 $*p < 0.05$, $***p < 0.001$.

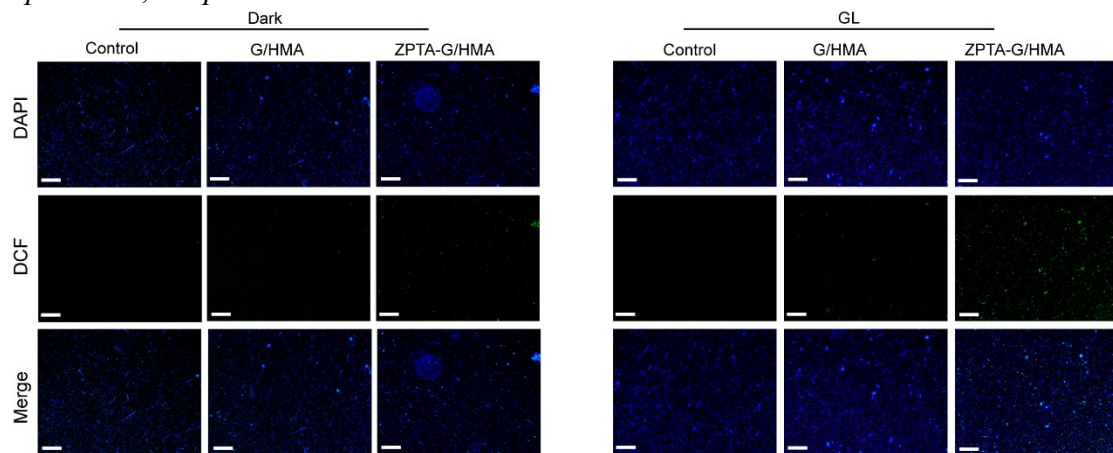


Figure S18. Fluorescence staining of ROS released from *E. coli* after incubation with different samples with/without GL irradiation. Scale bar = 50 μm .

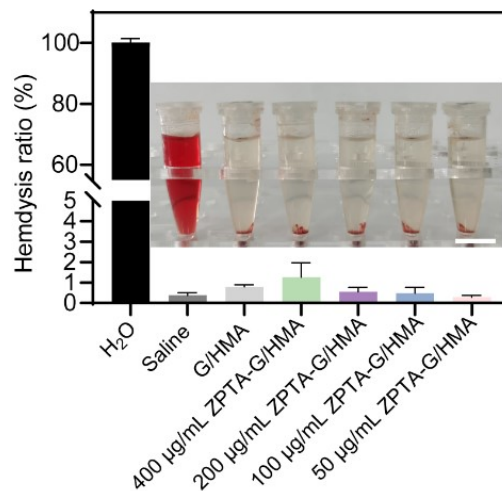


Figure S19. Hemolysis rates of RBCs co-cultured with G/HMA and different concentrations of ZPTA-G/HMA. The inset shows representative optical pictures. Scale bar = 2 cm. Data are means \pm s.d. ($n \geq 3$).

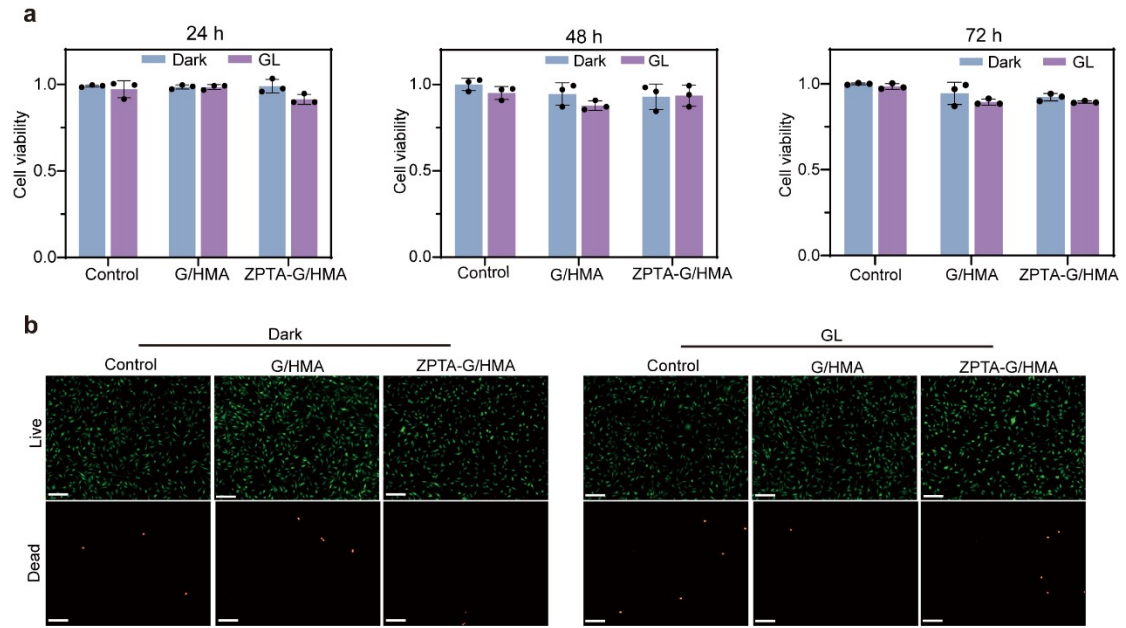


Figure S20. (a) Cell viabilities of L929 cells co-cultured with different treatments for 24, 48 and 72 h. (b) Live/dead cell staining. Live and dead cells were stained with green and red fluorescent stains, respectively. Scale bar = 200 μ m. Data are means \pm s.d. ($n \geq 3$).

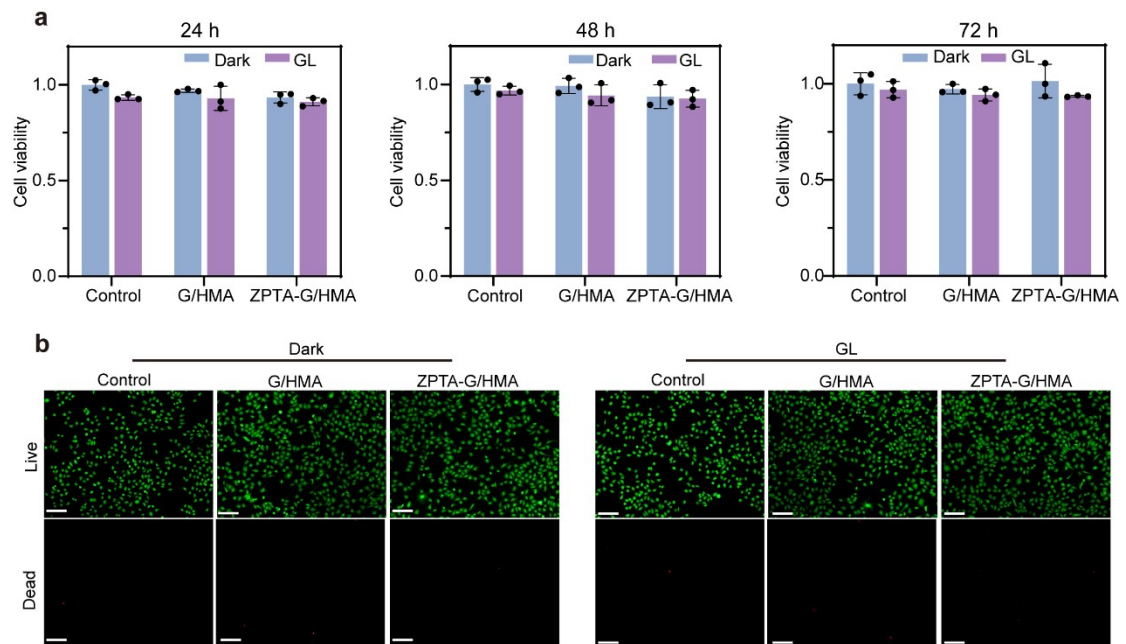


Figure S21. (a) Cell viabilities of HUVECs co-cultured with different treatments for 24 h, 48 h and 72 h. (b) Live/dead cell staining. Live and dead cells were stained with green and red fluorescent stains, respectively. Scale bar = 200 μ m. Data are means \pm s.d. ($n \geq 3$).

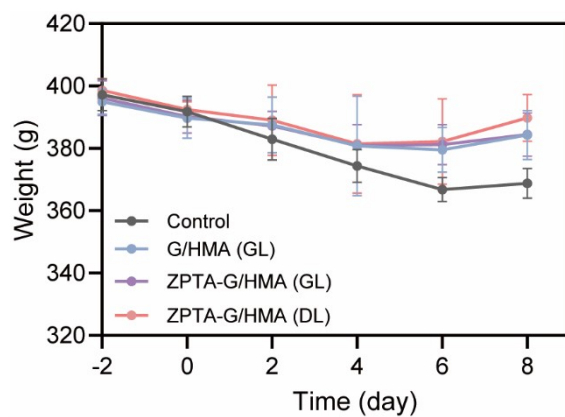


Figure S22. Body weight recordings of rats with different treatments. Data are means \pm s.d. ($n \geq 3$).

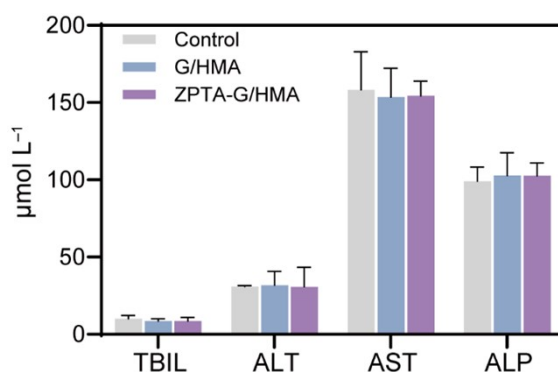


Figure S23. Serum levels of TBIL, ALT, AST and ALP of rats in different groups. Data are means \pm s.d. ($n \geq 3$).

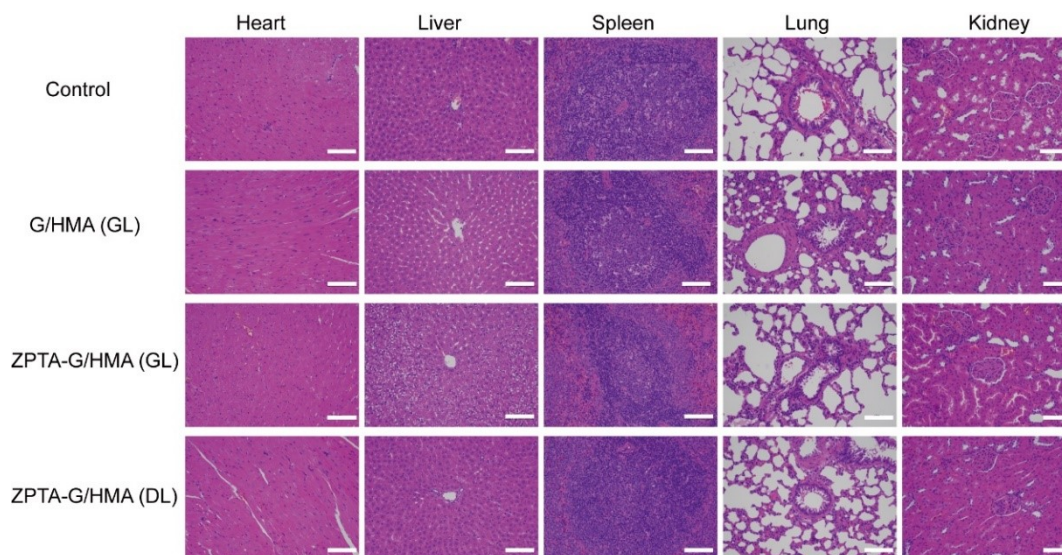


Figure S24. Histological sections of vital organs (heart, liver, spleen, lung and kidney) in different groups. Scale bar = 100 μ m.

Table S1. Routine blood tests of rats in different groups.

	Normal	Control	G/HMA (GL)	ZPTA-G/HMA (GL)	ZPTA-G/HAM (DL)
RBC	5.6-7.89 (10^{12} L^{-1})	5.33	7.57	7.04	7.28
WBC	2.9-15.3 (10^9 L^{-1})	73.0	17.2	8.5	5.7
PLT	100-1610 (10^9 L^{-1})	1522	1615	1588	1609
HGB	120-150 (g L^{-1})	174	159	137	151
HCT	36-46 (%)	34.6	47.0	41.8	42.0
MCH	16-23.1 (pg)	20.0	20.2	19.4	20.6
MCHC	300-341 (pg)	327	327	327	328
MCV	53-68 (fL)	65.0	62.0	59.5	62.9
Lymph#	2.6-13.5 (10^9 L^{-1})	26.7	10.1	5.4	3.7
Mon#	0.0-0.5 (10^9 L^{-1})	2.2	0.5	0.3	0.2